Self-Assembled Monolayers of Dendron Thiols for Electrodeposition of Gold Nanostructures: Toward Fabrication of Superhydrophobic/Superhydrophilic Surfaces and pH-Responsive Surfaces

Yugui Jiang, Zhiqiang Wang, Xi Yu, Feng Shi, Huaping Xu, and Xi Zhang*

Key Lab of Organic Optoelectronics & Molecular Engineering, Department of Chemistry, Tsinghua University, Beijing 100084, People's Republic of China, and Key Lab for Supramolecular Structure and Materials, College of Chemistry, Jilin University, Changchun 130023, People's Republic of China

Mario Smet and Wim Dehaen

Department of Chemistry, University of Leuven, Celestijnenlaan B-200F, 3001 Heverlee, Leuven, Belgium

Received October 11, 2004. In Final Form: December 17, 2004

This paper describes the fabrication of surfaces with different wettability, superhydrophobic/superhydrophilic, and pH-responsive properties. We used a self-assembled monolayer (SAM) of a dendron thiol as the underlying surface for electrodeposition of gold nanostructures. After this modification with a SAM of *n*-dodecanethiol or 11-mercaptoundecanol, the surface shows remarkable superhydrophobic properties with a contact angle of about 155° and a tilt angle of less than 2° or superhydrophilic properties with a contact angle of about 0°, respectively. Moreover, a large-scale pH-responsive surface was obtained by modification with 2-(11-mercaptoundecanamido)benzoic acid (**7**) (MUABA). The pH-responsive behavior was amplified by using rough surfaces.

1. Introduction

Since the origin of the self-cleaning property of lotus leaves has been revealed, the possibility to mimic lotus leaves and artificially make self-cleaning surfaces has generated increasing interest. A self-cleaning surface is a superhydrophobic surface with a contact angle (CA) larger than 150° and a tilt angle (TA) of less than 5°. Numerous methods have been used to create such a superhydrophobic surface, including plasma fluorination,[1] chemical vapor deposition,[2] reconformation of polymers,[3] electrodeposition on polyelectrolyte multilayer,[4] sol−gel method, and others.[5−7] In particular, from these methods we find that both the chemical modification (low surface free energy) and the surface structure (surface roughness) are very important factors determining the surface wetting properties. Consequently, the versatility of these methods makes them attractive for a number of areas including protective coating[8] and microfluidic devices.[9]

Up to now, there have been many types of substrates with different functionality used to fabricate such self-cleaning surfaces. We wished to determine if a self-assembled monolayer (SAM) of a dendron thiol on gold could be used as an underlying surface for fabricating gold surfaces with different wettability, since dendrimers,[10−12] regular branched macromolecules with structures precisely controlled at the molecular level, are promising candidates and building blocks for nanofabrication and nanodevices on a surface. In our previous work, we have reported a series of surface-bound dendron thiols and studied the factors that control the surface morphology of SAMs of those dendron thiols on a Au surface.[13−16] Herein, we attempt to use the SAM of dendron thiols as a matrix of electrodeposition for the fabrication of gold nanostructures. And as-prepared gold surfaces prepared by such an approach and the availability of a large number of thiol molecules with different chemical properties might represent an easy way to study the wetting of surfaces, combining modification of low surface free energy coating and surface roughness.

In addition, a stimuli-responsive surface, which can change its surface property depending on the external stimuli of environment at different conditions, e.g., electric

(1) Woodward, I.; Schofield, W. C. E.; Roucoules, V.; Badyal, J. P. S. *Langmuir* **2003**, *19*, 3432.
(2) Lau, K. K. S.; Bico, J.; Teo, K. B. K.; Chhowalla, M.; Amaratunga, G. A. J.; Milne, W. I.; Mckinley, G. H.; Gleason, K. K. *Nano Lett.* **2003**, *3*, 1701.
(3) Feng, L.; Song, Y. L.; Zhai, J.; Liu, B. Q.; Xu, J.; Jiang, L.; Zhu, D. B. *Angew. Chem., Int. Ed.* **2003**, *42*, 800.
(4) Zhang, X.; Shi, F.; Yu, X.; Liu, H.; Fu, Y.; Wang, Z. Q.; Jiang, L.; Li, X. Y. *J. Am. Chem. Soc.* **2004**, *126*, 3064.
(5) Tsujii, K.; Yamamoto, T.; Onda, T.; Shibuichi, S. *Angew. Chem., Int. Ed. Engl.* **1997**, *36*, 1011.
(6) Nakajima, A.; Fujishima, A.; Hashimoto, K.; Watanabe, T. *Adv. Mater.* **1999**, *11*, 1365.
(7) Tadanaga, T.; Morinaga, J.; Matsuda, A.; Minami, T. *Chem. Mater.* **2000**, *12*, 590.
(8) Alessandrini, G.; Aglietto, M.; Castelvetro, V.; Ciardelli, F.; Peruzzi, R.; Toniolo, L. *J. Appl. Polym. Sci.* **2000**, *76*, 962.
(9) Lam, P.; Wynne, K. J. K.; Wnek, G. E. *Langmuir* **2002**, *18*, 948.
(10) Grayson, O. S. M.; Fréchet, J. M. J. *Chem. Rev.* **2001**, *101*, 3819.
(11) van Manen, H. J.; van Veggel, F. C. J. M.; Reinhoudt, D. N. *Top. Curr. Chem.* **2001**, *217*, 121.
(12) Scott, W. J.; Ye, H.; Henriquez, R. R.; Crooks, R. M. *Chem. Mater.* **2003**, *15*, 3873.
(13) Dong, B.; Huo, F. W.; Zhang, L.; Yang, X. Y.; Wang, Z. Q.; Zhang, X.; Gong, S. Y.; Li, J. H. *Chem. Eur. J.* **2003**, *9*, 2331.
(14) Zhang, L.; Zou, B.; Dong, B.; Huo, F. W.; Zhang, X.; Chi, L. F.; Jiang, L. *Chem. Commun.* **2001**, 1906.
(15) Zhang, L.; Huo, F. W.; Wang, Z. Q.; Wu, L. X.; Zhang, X.; Höppener, S.; Chi, L. F.; Fuchs, H.; Zhao, J. W.; Niu, L.; Dong, S. J. *Langmuir* **2000**, *16*, 3813.
(16) Bo, Z. S.; Zhang, L.; Zhao, B.; Zhang, X.; Shen, J. C.; Höppener, S.; Chi, L. F.; Fuchs, H. *Chem. Lett.* **1998**, *27*, 1197.

10.1021/la047491b CCC: $30.25
Published on Web 02/03/2005

field,[17] thermal treatment,[18] etc., has attracted great interest of scientists. The stimuli responsiveness will be essential to control the surface physical properties, such as surface friction and surface wettability. Feng et al. and Sun et al. have reported that a ZnO_2 rough surface and a PNIPAAm-modified rough surface undergo a wettability transition from superhydrophobicity to superhydrophilicity upon UV illumination and thermal treatment, respectively.[19,20] Controlling the macroscopic physical properties of a surface, particularly the surface wettability by altering the pH, is especially interesting and fundamentally important for many material and biomaterial applications. Therefore, we designed and synthesized 2-(11-mercaptoundecanamido)benzoic acid (**7**) (MUABA) and investigated if it can be used for fabricating pH-responsive surfaces by the manipulation of surface free energy with pH.

2. Experimental Section

Materials. Decanethiol (C_{10}−SH, Fluka), dodecanethiol (C_{12}−SH, Fluka), 11-mercaptoundecanoic acid (HOOC−C_{10}−SH, Aldrich), and 11-mercaptoundecanol (HO−C_{11}−SH, Aldrich) were commercially obtained and used as received. Other chemicals were analytical-grade reagents and were used as received. The Fréchet-type dendron bromide was synthesized according to the literature.[21] The carboxyl-terminated dendron thiol was prepared from the reaction of the corresponding dendron bromide **1**, by using thioacetic acid,[22] followed by hydrolysis of both the focal point and the terminal group (Scheme 1). Dendron thiol **3** was characterized by ^{1}H NMR, ^{13}C NMR, LC-TOF-MS, and FT-IR. The synthesis of mercaptoalkyl derivative 2-(11-mercaptoundecanamido)benzoic acid (**7**) (MUABA) is shown in Scheme 2, which can be used for modification of pH-responsive wettability.

Synthesis of Second Generation Dendron Thioacetate $(CH_3OOC)_4$−[G-2]−$SCOCH_3$ (2). Dendron **1** (0.20 g, 0.19 mmol) was dissolved in 10 mL of dichloromethane, and the solution was cooled in an ice bath. The solution was stirred while triethylamine (80 μL, 0.58 mmol) and thioacetic acid (60 μL, 0.85 mmol) were added slowly. The solution was stirred for an additional 4 h at room temperature. Then, about 150 mL of dichloromethane was added to the reaction mixture and the resulting solution was washed three times with water. The organic layer was dried with anhydrous sodium sulfate, and the solvent was removed by evaporation in vacuo. The white crude product obtained was purified by column chromatography on silica gel using dichloromethane/diethyl ether (v/v = 10:1) as the eluent. Dendron thioacetate **2** ($C_{59}H_{54}O_{15}S$) (0.18 g, 0.17 mmol) was obtained as a white solid (90%). ^{1}H NMR (500 MHz, $CDCl_3$): δ (ppm) 8.05 (d, 8H, *o*-H $COOCH_3$), 7.48 (d, 8H, *m*-H $COOCH_3$), 6.66−6.44 (m, 9H, Ar−H), 5.10 (s, 8H, Ar−CH_2O-), 4.94 (s, 4H, Ar−CH_2O-), 4.04 (s, 2H, Ar−CH_2SCO-), 3.92 (s, 12H, −$COOCH_3$), 2.33 (s, 3H, −$SCOCH_3$).

Synthesis of Second Generation Dendron Thiol $(HOOC)_4$−[G-2]−SH (3). Thioacetate **2** (0.20 g, 0.19 mmol) was suspended in a mixture (60 mL) of 1 M NaOH(aq) and tetrahydrofuran (v/v = 1:2). The suspension was stirred at 45 °C under nitrogen for 24 h. After evaporation of tetrahydrofuran under reduced pressure, the resulting solution was washed three times with dichloromethane. The above solution was acidified with a 38% aqueous solution of hydrochloric acid. The white solid precipitate was filtered and washed several times with water,

Scheme 1. The Synthetic Process of Carboxyl-Terminated Polyaryl Ether Dendron Thiol, $(HOOC)_4$−G2−SH[a]

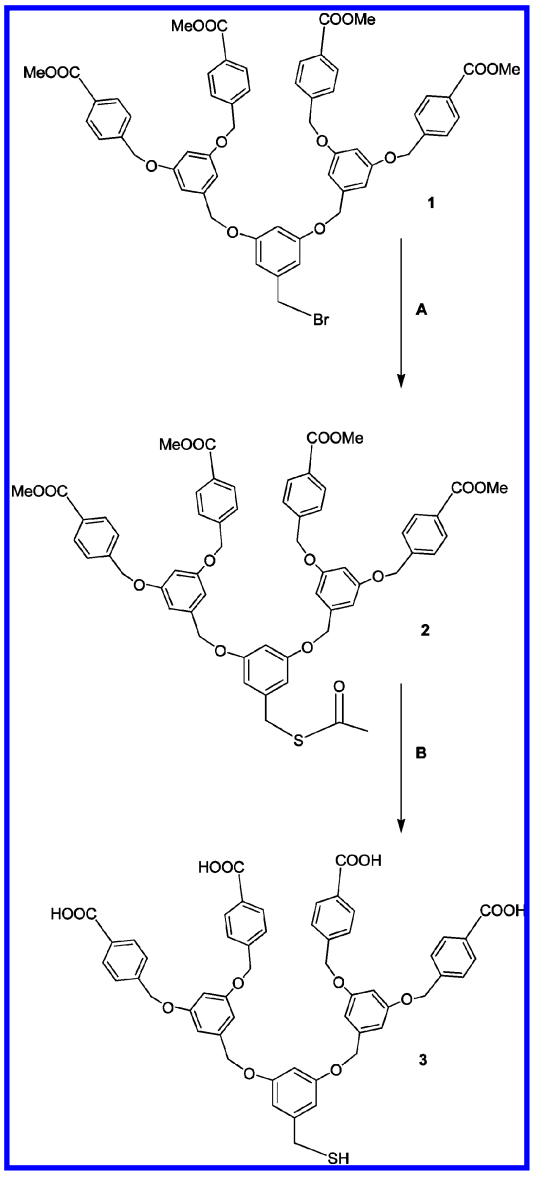

[a] Key: (A) $N(Et)_3$, CH_3COSH; (B) (a) NaOH, (b) HCl.

Scheme 2. The Synthetic Process of the pH-Responsive Molecule 2-(11-Mercaptoundecanamido)benzoic Acid (7) (MUABA)

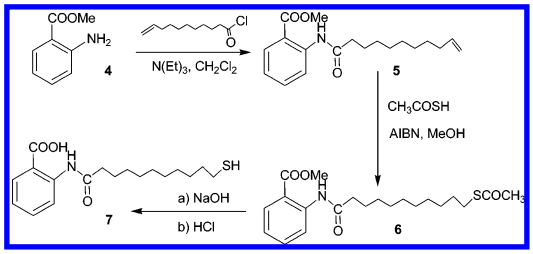

then dendron thiol **3** ($C_{53}H_{44}O_{14}S$) (0.14 g, 0.15 mmol) was obtained as a white solid (80%). ^{1}H NMR (500 MHz, DMSO): δ (ppm) 12.97 (s, 4H, −COOH), 7.96 (d, 8H, *o*-H COOH), 7.55 (d, 8H, *m*-H COOH), 6.73−6.51 (m, 9H, Ar−H), 5.18 (s, 8H, Ar−CH_2O-), 5.00 (s, 4H, Ar−CH_2O-), 3.65 (d, 2H, Ar−CH_2S-), 2.86 (t, 1H, −SH). ^{13}C NMR (125 MHz, DMSO): δ (ppm) 166.9 (C=O), 159.3, 143.7, 141.9, 139.5, 129.3 (Ar, tertiary carbon), 130.1, 127.3, 107.3, 106.6, 101.1, 100.1 (Ar−H, secondary carbon), 69.0, 68.7 (−CH_2O−), 27.8 (−CH_2S−). The DEPT (distortionless enhancement by polarization transfer)-135 method was utilized to

(17) Lahann, J.; Mitragotri, S.; Tran, T.; Kaido, H.; Sundaram, J.; Choi, I. S.; Hoffer, S.; Somorjai, G. A.; Langer, R. *Science* **2003**, *299*, 371.
(18) Crevoisier, D.; Fabre, P.; Corpart, J.; Leibler, L. *Science* **1999**, *285*, 1246.
(19) Feng, X. J.; Feng, L.; Jin, M. H.; Zhai, J.; Jiang, L.; Zhu, D. B. *J. Am. Chem. Soc.* **2004**, *126*, 62.
(20) Sun, T. L.; Wang, G. J.; Feng, L.; Liu, B. Q.; Ma, Y. M.; Jiang, L.; Zhu, D. B. *Angew. Chem., Int. Ed.* **2004**, *43*, 357.
(21) Hawker, C. J.; Wooley, K. L.; Fréchet, J. M. J. *J. Chem. Soc., Perkin Trans 1* **1993**, 1287.
(22) Tam-Chang, S.-W.; Biebuyck, H. A.; Whitesides, G. M.; Jeon, N.; Nuzzo, R. G. *Langmuir* **1995**, *11*, 4371.

differentiate the different types of carbon atoms in ^{13}C NMR. LC-TOF-MS: $[M - H^-]$ (*m/z*) found 935.549, calcd 935.97. FT-IR (ν_{max}/cm^{-1}, CaF_2) 2916, 2848 (CH_2), 1691 (C=O), 1597 (Ar C=C), 1450 (CH_2), 1159 (Ar−O), 1053 (C−O).

Synthesis of Methyl 2-Undec-10-enamidobenzoate (5). Methyl anthranilate (**4**) (3.5 g, 23 mmol) and triethylamine (3.5 g, 35 mmol) were dissolved in dichloromethane (80 mL). 10-Undecenoyl chloride (5.6 g, 28 mmol) was added slowly to the above solution under constant stirring. The solution was further stirred at room temperature during 1 h. The solvent was evaporated under reduced pressure, and the residue was dissolved in diethyl ether (80 mL). The organic layer was washed with brine (2 × 50 mL), dried over magnesium sulfate, and evaporated under reduced pressure. The crude product was purified by column chromatography on silica gel using dichloromethane as the eluent yielding **5** ($C_{19}H_{27}NO_3$) as a white powder (6.2 g, 85%). ^1H NMR (300 MHz, $CDCl_3$): δ (ppm) 11.07 (s, 1H, NH), 8.74 (d, J = 7 Hz, 1H, 6-H), 8.02 (d, J = 7 Hz, 1H, 3-H), 7.54 (t, J = 7 Hz, 1H, 4-H), 7.06 (t, J = 7 Hz, 1H, 5-H), 5.84−5.74 (m, 1H, =CH), 5.03−4.91 (m, 2H, $=CH_2$), 3.92 (s, 3H, CH_3), 2.44 (t, J = 7.3 Hz, 2H, $COCH_2$), 2.07−2.00 (m, 2H, $=CHCH_2$), 1.78−1.70 (m, 2H, $COCH_2CH_2$), 1.37−1.31 (m, 10H, rest CH_2). ^{13}C NMR (75 MHz, $CDCl_3$): δ (ppm) 172.7, 169.1, 142.1, 139.5, 135.1, 131.2, 122.7, 120.7, 115.1, 114.5, 52.7, 39.1, 34.2, 29.69, 29.66, 29.58, 29.46, 29.29, 25.9. MS (CI): $[M + H^+]$ (*m/z*) found 318, calcd 318.43.

Synthesis of Methyl 2-(11-(Acetylthio)undecanamido)-benzoate (6). Compound **5** (0.95 g, 3.0 mmol), thioacetic acid (1.0 g, 13 mmol), and AIBN (50 mg, 30 mmol) were dissolved in methanol (700 mL) under argon atmosphere. The solution was irradiated for 8 h with a mercury lamp through Duran glassware. After evaporation of the solvent under reduced pressure, the product was purified by column chromatography on silica gel with dichloromethane as the eluent yielding **6** ($C_{21}H_{31}NO_4S$) as a white powder (1.0 g, 88%). ^1H NMR (300 MHz, $CDCl_3$): δ (ppm) 11.06 (s, 1H, NH), 8.74 (d, J = 7 Hz, 1H, 6-H), 8.00 (d, J = 7 Hz, 1H, 3-H), 7.52 (t, J = 7 Hz, 1H, 4-H), 7.04 (t, J = 7 Hz, 1H, 5-H), 3.91 (s, 3H, CH_3), 2.85 (t, J = 6.0 Hz, 2H, SCH_2), 2.43 (t, J = 7.3 Hz, 2H, $NHCOCH_2$), 2.30 (s, 3H, $-SCOCH_3$), 1.77−1.28 (m, 16H, rest CH_2). ^{13}C NMR (75 MHz, $CDCl_3$): δ (ppm) 196.1, 172.5, 169.0, 142.1, 134.9, 131.1, 122.6, 120.6, 115.0, 52.6, 39.0, 30.9, 29.84, 29.73, 29.70, 29.63, 29.50, 29.44, 29.41, 29.12, 25.8. MS (CI): $[M + H^+]$ (*m/z*) found 394, calcd 394.55.

Synthesis of 2-(11-Mercaptoundecanamido)benzoic Acid (7) (MUABA). Thioacetate **6** (0.12 g, 0.31 mmol) was dissolved in a mixture of methanol (3 mL) and THF (1 mL). After argon was bubbled through the mixture for 10 min, an aqueous NaOH solution (1 M, 1 mL) was added. The mixture was stirred under argon atmosphere at room temperature for 16 h. After addition of aqueous HCl (1 M, 1.1 mL) under argon atmosphere, the solution was extracted with dichloromethane (10 mL). After being dried with magnesium sulfate, the solvent was removed under reduced pressure and the crude product was purified by column chromatography on silica gel with dichloromethane/ethyl acetate, (v/v = 3:1) as the eluent yielding **7** ($C_{18}H_{27}NO_3S$) as a white powder (78 mg, 76%). ^1H NMR (300 MHz, $CDCl_3$) δ (ppm) 10.96 (s, 1H, NH), 8.77 (d, J = 7 Hz, 1H, 6-H), 8.13 (d, J = 7 Hz, 1H, 3-H), 7.52 (t, J = 7 Hz, 1H, 4-H), 7.12 (t, J = 7 Hz, 1H, 5-H), 2.54−2.45 (m, 4H, $COCH_2$, CH_2SH), 1.79−1.29 (m, 16H, rest CH_2). ^{13}C NMR (75 MHz, $CDCl_3$): δ (ppm) 198.80, 198.42, 173.07, 172.43, 170.98, 142.55, 136.08, 132.13, 123.01, 121.00, 114.23, 39.10, 34.39, 30.10, 29.84, 29.75, 29.69, 29.54, 29.43, 28.74, 25.90, 25.04. MS (ES): $[M + Na^+]$ (*m/z*) found 360.3, calcd 360.47.

Preparation of the Gold Substrates. After a thorough cleaning, a quartz or glass substrate was precoated with 6 nm of chromium followed by 130 nm of gold, both evaporated at a pressure of 5 × 10^{-6} mbar from a resistively heated tungsten boat. The resulting gold substrates for STM measurements were further flame annealed at about 1000 K for about 1 min,[23] such treatment often produced large areas of Au(111) terraces, often extending over thousands of angstroms.

Preparation of the Self-Assembled Monolayer (SAM) on Gold. The gold-coated substrates for electrodeposition measurements were dipped into the dendron thiol $(HOOC)_4-[G\text{-}2]-SH$ solution at room temperature for at least 24 h, while the gold-coated substrates for STM measurements, after flame-annealing and cooling to room temperature, were dipped into an ethanolic solution of dendron thiol $(HOOC)_4-[G\text{-}2]-SH$ (1 mM) at 50 °C for at least 8 h. Then the SAMs on gold substrate were rinsed extensively with pure ethanol and dried in a stream of dry nitrogen before characterization. For COOH-terminated SAMs, they were rinsed sequentially with pure ethanol, 10% acetic acid, and ethanol and then dried with a stream of nitrogen.

General Techniques. ^1H NMR and ^{13}C NMR spectra were recorded with $CDCl_3$ and DMSO solutions on a Bruker Advance 500 spectrometer using TMS as the internal reference. FT-IR spectra and infrared reflection−absorption spectra (IR-RAS) were collected with an IFS-66v/S FT-IR spectrometer (Bruker) with a MCT detector cooled with liquid nitrogen. X-ray photoelectron spectroscopy was performed on a VG ESCALAB MK II spectrometer with a Mg Kα X-ray source (1253.6 eV). The base pressure in the analysis chamber during spectral acquisition was 3 × 10^{-7} Pa. The spectra were collected using the pass energy of 50 eV with SAM-covered gold slides as the substrate and calibrated by referencing to the binding energy of C_{1s}. Molecular weights of the compounds were measured on a QSTAR LC-MS mass spectrometer. Scanning tunneling microscopy (STM) measurements were carried out with a commercial instrument (Digital Instruments, Multimode Nanoscope IIIa) at room temperature in air. STM tips were prepared from Pt−Ir wire by the mechanical cutting method. Tunneling parameters of 750 mV (bias voltage) and 500 pA (current setpoint) were used for taking images if not indicated otherwise. Scanning electron microscopy (SEM) images were recorded on a JEOL JSM-6700F at 10.0 kV. Water contact angle values were acquired at room temperature using an optical contact angle measuring device (OCA 20, Dataphysics Instruments GmbH) by sessile drop and tilting plate measuring method. A video system with CCD camera (CCD resolution 768 × 576 pixels) and halogen lighting with continuous adjustable intensity without hysteresis for homogeneous back lighting were used to image the water droplet. Ellipse fitting was selected as the default calculation method in the sessile method. The test liquid chosen to evaluate hydrophobicity was deionized water. In the case of superhydrophobic surfaces, in each measurement a 4 μL droplet was dispensed onto the substrate under investigation, and the water droplet rolled off the surface easily. For other surfaces with a contact angle of below 150°, a droplet size of 2 μL was often used to measure the contact angle more accurately. A water droplet size of 4 μL was used for tilt angle measurements, if not otherwise indicated.

3. Results and Discussion

3.1. Electrodeposition of Gold Nanostructures. The formation of gold nanostructures can be adjusted by controlling the time of electrodeposition. Figure 1 shows SEM images of the gold nanostructures formed on the SAM of the dendron thiol $(HOOC)_4-G2-SH$ by electrodeposition at −200 mV in a $HAuCl_4/H_2SO_4$ mixture electrolyte for different electrodeposition time. As indicated by SEM observation shown in this figure, a few uniform gold nanostructures form at the very beginning of the electrodeposition; thereafter, with extension of the electrodeposition time, the surface density of the gold nanostructures increases with a gradual augmentation of the particle size. As a result, the surface roughness also becomes larger with the increase of the time of electrodeposition. In addition, the morphology of the electrodeposited gold nanostructures formed is found to be potential controlled. We have changed the potential for electrodeposition and found that upon electrodeposition at −400 mV discrete gold particles were formed, as shown in Figure 2a, which is obtained under the same conditions except the electrodeposition potential, but their shape is quite different from that shown in Figure 1d.

There are reasons why the dendron thiol has been chosen as the underlying surface for electrodeposition.

(23) Haiss, W.; Lackey, D.; Sass, J. K.; Besocke, K. H. *J. Chem. Phys.* **1991**, *95*, 2193.

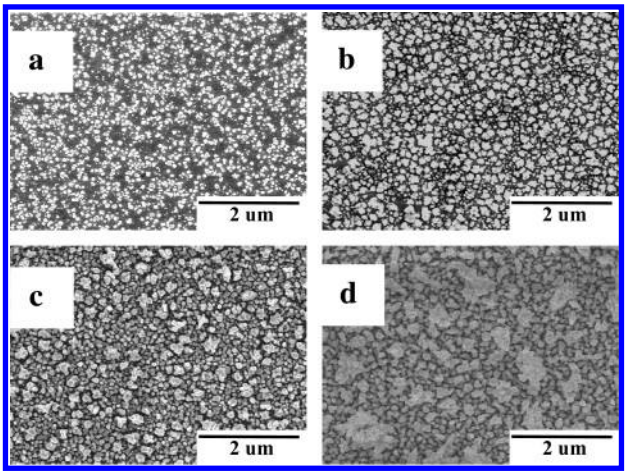

Figure 1. SEM images of gold nanostructures formed on the $(HOOC)_4-G2-SH$ SAM-covered substrate by electrodeposition at −200 mV (vs Ag/AgCl) in a mixture electrolyte of H_2SO_4 (0.5 M) and $HAuCl_4$ (1 mg/mL) for different times. Electrodeposition times were (a) 10 s, (b) 300 s, (c) 800 s, and (d) 1600 s.

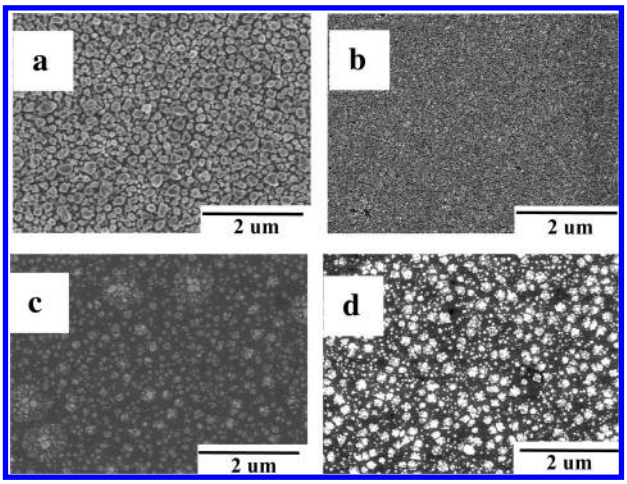

Figure 2. (a) SEM images of electrodeposited gold nanostructures formed on the SAM-covered substrate by electrodeposition at −400 mV (vs Ag/AgCl). SEM images of gold nanostructures formed on different surfaces by electrodeposition at −200 mV (vs Ag/AgCl) in an electrolyte mixture of H_2SO_4 (0.5 M) and $HAuCl_4$ (1 mg/mL) and at the same electrodeposition time of 100 s. The underlying surfaces are (b) no SAM, bare gold substrate, (c) $HOOC-C_{10}-SH$, and (d) $(HOOC)_4-G2-SH$.

First, electrodeposition on a bare gold substrate (Figure 2b) results in small gold nanostructures. The process of electrodeposition on a bare gold substrate is too quick to allow efficient control, and as-prepared surface of gold nanostructures are not rough enough. Second, the process of electrodeposition on ordered SAM-modified gold substrates, e.g., 11-mercaptoundecanoic acid ($HOOC-C_{10}-SH$) SAMs, is slower, because such an ordered SAM on gold results in high resistance. As a consequence, the gold nanostructures did not cover completely the underlying surface after the same electrodeposition time (Figure 2c). However, in the case of dendron thiol $(HOOC)_4-[G-2]-SH$ SAMs on a gold substrate, the presence of many pitlike defects in the SAM enable relatively easy charge transfer (Figure 2d). Therefore, such SAMs provide a good matrix to fabricate the rough surface of the gold nanostructures, thus making them suitable to mimic lotus leaves with self-cleaning properties.

3.2. Fabrication of Superhydrophobic and Superhydrophilic Surfaces. Surface wetting properties rely on the combination of surface structure and chemical modification. After modification of the surface covered

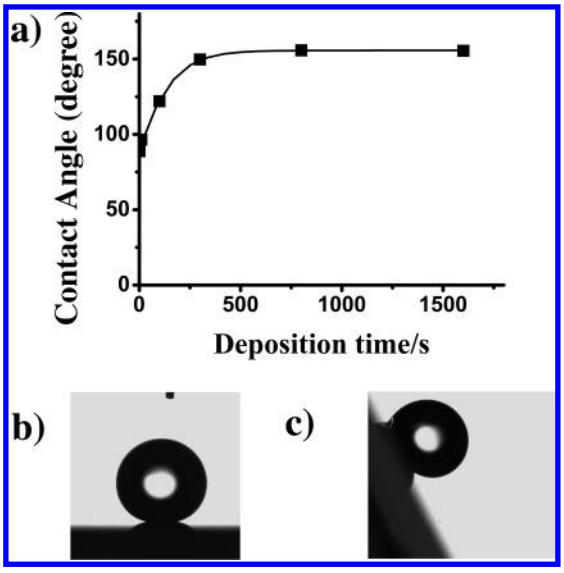

Figure 3. (a) Water contact angle measurements on the surface of *n*-dodecanethiol-modified electrodeposited gold nanostructures as a function of the duration of electrochemical deposition at −200 mV (vs Ag/AgCl). (b) The shape of a water droplet on the surface of electrodeposited gold nanostructures for electrodeposition time of 1600 s (4 μL droplet size). Contact angle about 155°. (c) Static shape of a water droplet (TA > 60°) on the tilt surface of electrodeposited gold nanostructures for an electrodepositon time of 300 s (4 μL droplet size).

with gold nanostructures with low surface free energy chemicals, e.g., *n*-dodecanethiol ($C_{12}-SH$), the surface CA increases gradually with the increase of electrodeposition time, reflecting the evolution from less hydrophobic to superhydrophobic (Figure 3a). When electrodeposition time is as high as 1600 s, the surface shows a CA of about 155° (Figure 3b) and a TA of below 2°, using water as an indicator (4 μL droplet size). TA reflects the difference between the advancing and receding CA (CA hysteresis), and the low TA indicates that water droplets roll off easily. Therefore, a kind of self-cleaning surface has been fabricated successfully by combination of electrodeposition (surface structure) and postmodification (chemical modification).

To understand the origin of the observed superhydrophobicity, we have described the CA in terms of the Cassie equation,[24] $\cos\theta_r = f_1 \cos\theta - f_2$, in which f_1 and f_2 are the fractions of solid surface and air in contact with liquid, respectively. θ_r and θ are the CAs on the SAM of *n*-dodecanethiol with a rough surface covered with electrodeposited gold nanostructures (155°) and with a smooth gold surface (107°[25]), respectively. Since $f_1 + f_2 = 1$, f_1 and f_2 are calculated to be 0.13 and 0.87. The high value of f_2 suggests that the very large fraction of air trapped in the interspaces among the electrodeposited gold nanostructures is responsible for the superhydrophobicity.

Figure 3a shows that a value of 149° has already been reached for CA after an electrodeposition time of 300 s. The surface cannot, however, be termed as a self-cleaning surface, because the TA is beyond 60°. In other words, the water droplet does not roll off easily (Figure 3c), though the surface is superhydrophobic. For a electrodeposition time of 800 s, the CA is already as high as 155°, but the TA is still beyond 10°. As discussed above, when the electrodeposition time is 1600 s, the formed gold nanostructures show a CA of 155° and a TA less than 2°, thus

(24) Cassie, A. B. D. *Trans. Faraday Soc.* **1948**, *44*, 11.
(25) Michael, K. E.; Vernekar, V. N.; Keselowsky, B. G.; Meredith, J. C.; Latour, R. A.; García, A. J. *Langmuir* **2003**, *19*, 8033.

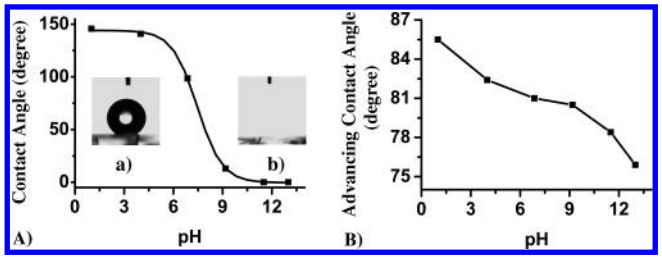

Figure 4. (A) The water contact angle as a function of pH on the rough surface of gold nanostructures at −200 mV (vs Ag/AgCl) with the electrodeposition time of 2400 s, after the modification of MUABA SAM. Inset: (a) The water droplet at pH = 1. Contact angle about 145°. (b) The water droplet at pH = 13. Contact angle near 0°. (B) The water advancing contact angle as a function of pH on a flat gold surface, after the modification of MUABA SAM.

meeting the requirement of a self-cleaning surface. The fact that TA becomes smaller and smaller with the extension of electrodeposition time is consistent with the gradual increase of surface roughness. It also agrees well with the simulation work of Johnson and Dettre[26] showing that the CA hysteresis on hydrophobic surfaces increases with increasing surface roughness in the low roughness region but decreases drastically when the roughness becomes large.

In addition, for gold nanostructures electrodeposited at −200 mV (vs Ag/AgCl) for 1600 s and modified with 11-mercaptoundecanol (HO−C_{11}−SH), the surface was found to exhibit superhydrophilic properties with a CA of close to 0°. The water droplet dispensed on the surface spreads immediately. To understand the origin of the superhydrophilicity, we describe the CA in terms of the Cassie hemiwicking model,[27] $\cos\theta_r = f_1\cos\theta + f_2$, in which f_1 and f_2 are the fractions of solid surface and liquid in the interspaces among the electrodeposited gold nanostructures in contact with water, respectively. θ_r and θ are the CAs on the SAM of HO−C_{11}−SH with a rough surface, assuming a sketchy value of 5° and of 25° on a smooth surface,[25] respectively. It can be deduced from this equation that increasing the fraction of liquid (f_2) decreases the CA of the rough surface (θ_r). According to the equation, the f_2 value of the rough surface with gold nanostructures is estimated to be as high as 0.96, resulting in the superhydrophilic surface.

3.3. pH-Responsive Wetting Properties. It is reported that polyethylene films can show a pH responsive wettability after modification with acylated anthranilate moieties through surface reaction.[28] Inspired by this work, we designed and synthesized the mercaptoalkyl derivative, 2-(11-mercaptoundecanamido)benzoic acid (**7**) (MUABA, Scheme 2). After modification of the rough surface with this compound, the rough surface of gold nanostructures exhibited a pH-responsive behavior (Figure 4A) with an exceptionally large change in CA as a function of the pH, from nearly superhydrophobic (CA of about 145°) to superhydrophilic (CA of near 0°) (Figure 4A). Though given the fact that the carboxylic acid groups at low pH can be protonated and relatively hydrophobic (−COOH) and at high pH present as carboxylate anions and more hydrophilic (−COO^-), the change of conformation may be essential for the large change of CA with pH.[28] Moreover, this change on rough surface (Figure 4A) is much larger than the one observed on flat gold surfaces (Figure 4B). Therefore it seems reasonable to conclude that the roughness of the gold nanostructures likely enhances the pH-responsive properties and, hence, results in the observed large-scale pH-responsive behavior, while leaving the morphology of the surface constant.

4. Conclusions

In conclusion, we have demonstrated that the SAM of dendron thiols can be used as an underlying surface for electrodeposition of gold nanostructures at the same time allowing the control of their size and shape by electrodeposition time and electrodeposition potential. Moreover, further modification of the gold nanostructures with either *n*-dodecanethiol or 11-mercaptoundecanol results in good superhydrophobic or superhydrophilic properties, respectively. It is anticipated that this research may open a route for fabrication of nanostructured materials and provide a way for mimicing lotus leaves, leading to the production of self-cleaning coatings. Furthermore, a large-scale pH-responsive surface was obtained by modification of gold with **7**. Compared to a flat gold surface, the roughness of the gold significantly enhanced the responsiveness of the anthranilic monolayer. These findings demonstrate that surface structure plays a significant role in the amplification of pH-responsive behavior, and this concept is expected to be also valid for other types of stimuli-responsive systems such as electrical potentials.

Acknowledgment. The authors thank the Major State Basic Research Development Program (Grant. No. G2000078102), 863 High-tech R&D Program (2003AA302140), Ministry of Education (key project, and 20020010006), and National Natural Science Foundation of China (20334010, 20473045) for financial support. The Flemish government is thanked for a bilateral grant (BIL02/03). M.S. thanks the F.W.O. Vlaanderen for a postdoctoral fellowship.

Supporting Information Available: Further details of preparation and characterization of self-assembled monolayers of dendron thiol $(HOOC)_4$−G2−SH on gold. This material is available free of charge via the Internet at http://pubs.acs.org.

LA047491B

(26) Johnson, R. E., Jr.; Dettre, R. H. *Adv. Chem. Ser.* **1963**, *No. 43*, 112.
(27) Bico, J.; Thiele, U.; Quéré, D. *Colloids Surf., A* **2002**, *206*, 41.
(28) Wilson, M. D.; Whitesides, G. M. *J. Am. Chem. Soc.* **1988**, *110*, 8718.